R. Sarao for comments and assistance and M. Saunders for scientific editing. We thank J. Collard and G. Koretzky for reagents. E.K.G. is supported by a scholarship from the Natural Sciences and Engineering Research Council (NSERC) of Canada. C.E.R. is a Principal Research Fellow of the Wellcome Trust, London. J.M.P. is supported by Amgen, grants from the Canadian Institutes for Health Research (CIHR), the National Cancer Institute of Canada (NCIC), the Premier's Research Excellence Award (PREA), and the Canadian Network for Vaccines and Immunotherapeutics of Cancer and Chronic Viral Disease (CANVAC). J.M.P. holds a Canadian Research Chair in Cell Biology.

13 June 2001; accepted 20 July 2001

Coupling of the TCR to Integrin Activation by SLAP-130/Fyb

Erik J. Peterson,[1,2] Melody L. Woods,[5] Sally A. Dmowski,[1] Geo Derimanov,[1,2] Martha S. Jordan,[1] Jennifer N. Wu,[1] Peggy S. Myung,[1] Qing-Hua Liu,[4] Jonathan T. Pribila,[5] Bruce D. Freedman,[4] Yoji Shimizu,[5] Gary A. Koretzky[1,3]*

SLAP-130/Fyb (SLP-76–associated phosphoprotein or Fyn-binding protein; also known as Fyb/Slap) is a hematopoietic-specific adapter, which associates with and modulates function of SH2-containing leukocyte phosphoprotein of 76 kilodaltons (SLP-76). T cells from mice lacking SLAP-130/Fyb show markedly impaired proliferation following CD3 engagement. In addition, the T cell receptor (TCR) in SLAP-130/Fyb mutant cells fails to enhance integrin-dependent adhesion. Although TCR-induced actin polymerization is normal, TCR-stimulated clustering of the integrin LFA-1 is defective in SLAP-130/Fyb–deficient cells. These data indicate that SLAP-130/Fyb is important for coupling TCR-mediated actin cytoskeletal rearrangement with activation of integrin function, and for T cells to respond fully to activating signals.

Following the engagement of lymphocyte surface receptors, adapter proteins play critical roles in regulating second messenger signaling cascades (*1*). T cell receptor (TCR) signaling (*2*) and murine thymocyte development (*3, 4*) require the presence of the hematopoietic adapter SLP-76 (SH2 domain containing Leukocyte Phosphoprotein of 76 kD). SLP-76 likely functions as a scaffold for multimolecular complexes that coordinate signaling. However, it is not fully understood how SLP-76 couples TCR-stimulated protein tyrosine kinase (PTK) activity with downstream signals. SLP-76 associates in a TCR-inducible fashion with SLAP-130/Fyb, another hematopoietic-specific adapter (*5, 6*). Although SLAP-130/Fyb has been implicated in T cell migration and rearrangement of the actin cytoskeleton (*7, 8*), overexpression studies seeking to define a functional role for SLAP-130/Fyb in TCR signaling have been inconclusive (*5, 6*).

To address the role of SLAP-130/Fyb in TCR signaling, we generated SLAP-130/Fyb–deficient mice (*9–12*). SLAP-130/Fyb mutant animals are born at expected Mendelian frequencies; the mice are viable, fertile, and show normal growth. Hematopoietic cellularity is normal with the exception of modest thrombocytopenia, a 50% reduction in splenic T cells, and mildly decreased thymocyte number (*13*). We found no differences between wild-type and SLAP-130/Fyb–deficient mice in subsets of thymocytes expressing developmental markers or coreceptors (*13*). Thus, SLAP-130/Fyb, unlike SLP-76, appears dispensable for orderly progression of T cell development.

Because a SLP-76–deficient T cell line exhibits uncoupling of TCR-stimulated protein tyrosine kinases (PTKs) from signals critical for cellular activation (*2*), we examined TCR-stimulated biochemical events in purified SLAP-130/Fyb$^{-/-}$ lymph node and splenic T cells. The earliest detectable biochemical event following engagement of the TCR is activation of members of several families of PTKs. SLAP-130/Fyb$^{-/-}$ T cells exhibit TCR-induced phosphorylation of SLP-76 and PLCγ-1 (Fig. 1A) similar to control cells. Downstream of PTK activation, MAPK up-regulation and calcium elevation are required elements in TCR-dependent cellular activation. Unlike SLP-76–deficient Jurkat cells, SLAP-130/Fyb$^{-/-}$-purified T cells display TCR-dependent MAPK phosphorylation with kinetics comparable to controls (Fig. 1B). We found no decrease in TCR-mediated calcium elevation either by ratiometric flow cytometric assay (Fig. 1C) or by microscopic digital imaging (*14*) of individual T cell fura-2 fluorescence (*15*). From these data, we conclude that SLAP-130/Fyb does not regulate TCR signaling either at the level of PTK activation or in the coupling of PTK activity with key cytoplasmic biochemical events.

TCR signaling results in transactivation of several gene products, including the surface antigens CD25 and CD69. We stimulated purified SLAP-130/Fyb$^{-/-}$ T cells with anti-CD3 for 18 hours, and assessed expression of both markers. Up-regulation of CD25, and to a lesser extent, of CD69, was markedly reduced in SLAP-130/Fyb$^{-/-}$ T cells com-

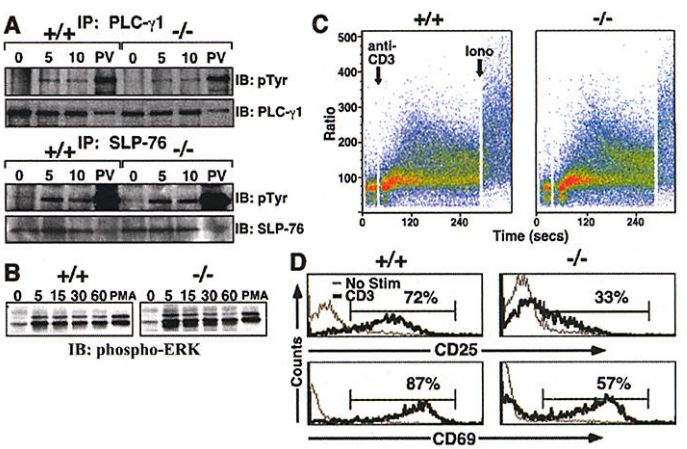

Fig. 1. Proximal signaling occurs in the absence of SLAP-130/Fyb, but early activation antigen expression is impaired. (**A**) Purified splenic T cells (*9–12*) were left unstimulated, or treated with soluble anti-CD3ε (500A2, 5 μg/ml, Pharmingen) for indicated minutes, or with pervanadate (PV) (1 mM $NaVO_4$, 1% H_2O_2) for 2 min. Cellular lysates were prepared in 1% NP-40, and were subjected to immunoprecipitation with anti-SLP-76 or anti-PLCγ1 (Upstate Biotechnology), followed by Western blotting with indicated antisera. In (**B**), cells were left unstimulated or treated with anti-CD3ε (500A2, 5 μg/ml) for the indicated times. Resolved cell lysates were interrogated with anti-phospho-ERK (New England Biolabs). For (**C**), purified lymph node T cells (*9*) were loaded with Indo-1 and stained with anti-CD3ε at 30°C, followed by stimulation with goat anti-hamster (10 μg/ml). Intracellular calcium elevations after TCR stimulation ("anti-CD3") or ionomycin ("Iono") were detected by ultraviolet laser flow cytometry. (**D**) Purified splenic T cells were cultured with platebound anti-CD3ε (2C11, 5 μg/ml) for 18 hours, stained with anti-CD69 or anti-CD25 (Pharmingen), and analyzed by FACS.

[1]The Abramson Family Cancer Research Institute, Departments of [2]Medicine and [3]Pathology and Laboratory Medicine, School of Medicine, and the [4]Department of Pathobiology, School of Veterinary Medicine, University of Pennsylvania, Philadelphia, PA, 19104, USA. [5]Department of Pathology and Laboratory Medicine, Center for Immunology, Cancer Center, University of Minnesota Medical School, Minneapolis, MN 55455, USA.

*To whom correspondence should be addressed. E-mail: koretzky@mail.med.upenn.edu

pared with controls (Fig. 1D). This result suggested suboptimal activation response to TCR engagement, despite intact proximal signaling in SLAP-130/Fyb$^{-/-}$ cells.

We next examined proliferation and interleukin-2 (IL-2) production as longer term parameters of T cell activation. A profound defect in the proliferative response of purified SLAP-130Fyb$^{-/-}$ T cells to anti-CD3ε stimulus (Fig. 2A) was observed. Costimulation of the mutant T cells with anti-CD28 slightly augmented, but did not restore anti-CD3-stimulated proliferation to wild-type levels. Addition of phorbol myristate acetate (PMA), a receptor-independent co-stimulus, partially rescued the proliferation defect (Fig. 2A), and stimulation of the mutant cells with PMA plus calcium ionophore produced proliferation comparable with wild-type (*15*). Similarly, a marked decrease in IL-2 production by purified SLAP-130/Fyb$^{-/-}$ T cells was apparent after stimulation with anti-CD3, or with anti-CD3 plus anti-CD28 (Fig. 2B). Stimulation with combined PMA and calcium ionophore elicited equivalent IL-2 production in SLAP-130/Fyb$^{-/-}$ and control T cells (Fig. 2B), suggesting no intrinsic IL-2 synthesis defect in the mutant.

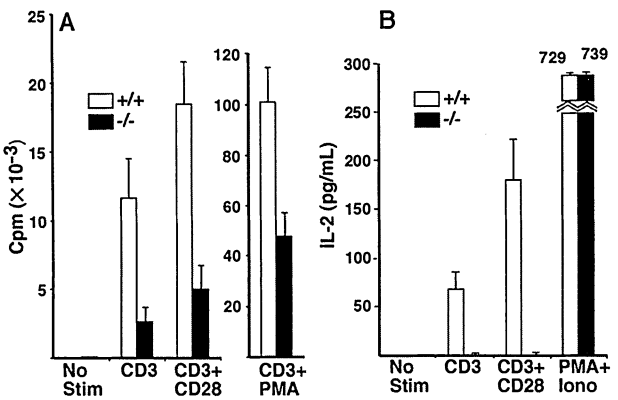

Fig. 2. SLAP-130/Fyb$^{-/-}$ T cells exhibit impaired proliferation and IL-2 production. **(A)** 10^5 purified splenic T cells were left unstimulated, or were cultured with anti-CD3ε (2C11, plate bound, 0.75 μg/ml) with anti-CD3ε plus soluble anti-CD28 (1 μg/ml), or anti-CD3ε plus PMA (20 ng/ml) for 48 hours. Proliferation was measured by ^{3}H-thymidine (ICN) uptake. **(B)** Purified T cells were stimulated under the indicated conditions for 40 hours (ionomycin, 200 ng/ml). IL-2 in culture supernatants was measured by ELISA (R&D Systems).

Lack of IL-2 production does not completely account for the proliferation defect in SLAP-130/Fyb$^{-/-}$ T cells, as addition of exogenous IL-2 only partially rescued CD3-induced proliferation. Interactions of integrins such as lymphocyte function-associated antigen–1 (LFA-1) with their cognate ligands have been shown to be critical for TCR-mediated responses (*16*). Moreover, SLAP-130/Fyb has been implicated in the regulation of integrin function (*8*). Accordingly, we explored a potential role for SLAP-130/Fyb in TCR-mediated activation of LFA-1–dependent adhesion to intercellular adhesion molecule–1 (ICAM-1) (*17*). Basal adhesion of unstimulated SLAP-130/Fyb$^{-/-}$ T cells to plate-bound ICAM-1 was comparable to that of wild-type cells (Fig. 3A). As in human T cells (*17, 18*), engagement of the TCR on wild-type murine T cells resulted in a rapid increase in LFA-1–dependent adhesion to mouse ICAM-1. In contrast, no increase in adhesion was seen following TCR stimulation of SLAP-130/Fyb$^{-/-}$ T cells. However, treatment of the SLAP-130/Fyb$^{-/-}$ cells with either PMA (Fig. 3A), which bypasses proximal TCR signaling events (*17, 18*), or with Mn^{2+} (*15*), which enhances LFA-1 activity through direct induction of LFA-1 conformational changes (*19*), induced comparable adhesion of control and SLAP-130/Fyb$^{-/-}$ T cells to ICAM-1. These results show that LFA-1 expressed on SLAP-130/Fyb$^{-/-}$ T cells can mediate adhesion to ICAM-1, but that enhanced cell adhesion after TCR ligation is defective. Similar impairment of TCR-, but not PMA- or Mn^{2+}-induced increases in adhesion to purified mouse vascular cell adhesion molecule–1 (VCAM-1), a ligand for the α4β1 and α4β7 integrins, was observed in SLAP-130/Fyb$^{-/-}$ T cells (*15*). The defect in TCR-induced adhesion of SLAP-130/Fyb$^{-/-}$ T cells to ICAM-1 is not due to altered LFA-1 expression, as similar levels of the CD11a (αL) subunit of LFA-1 are expressed on control and SLAP-130/Fyb$^{-/-}$ T cells (Fig. 3B).

Molecular events linking the TCR to LFA-1 activation include activation of phosphatidylinositol-3 kinase (PI-3K) and actin cytoskeletal rearrangement (*20*). We found no clear defect either in TCR-stimulated PI-3K enzymatic activity or in the phosphoryl-

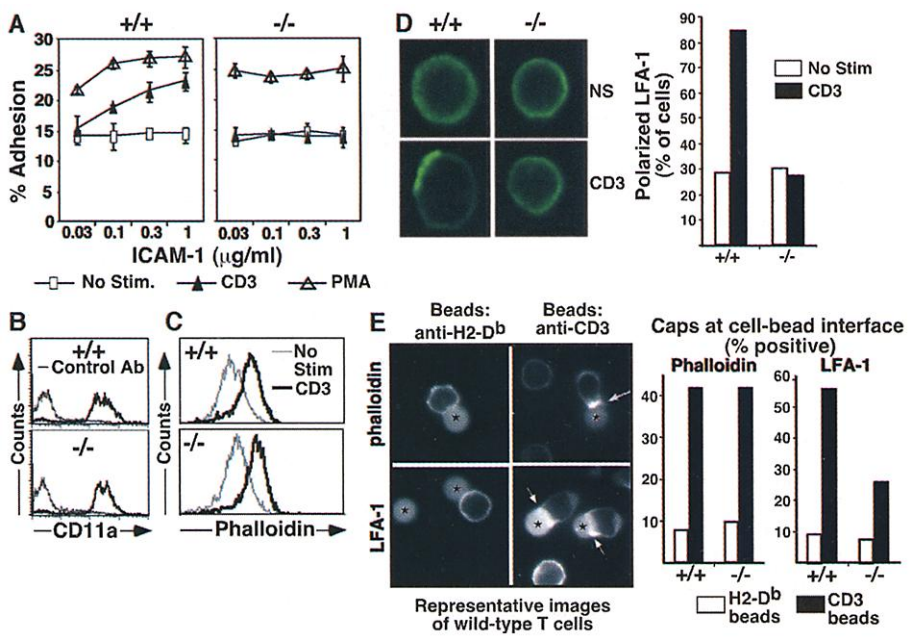

Fig. 3. SLAP-130/Fyb$^{-/-}$ T cells display defective TCR-induced adhesion to ICAM-1 and impaired LFA-1 lateral mobility. **(A)** Calcein-AM (Molecular Probes)–labeled B220-depleted splenocytes were exposed to anti-CD3ε (2C11, 2 μg/ml) and 1 μg/ml rabbit anti-hamster IgG or to PMA (10 ng/ml) and then incubated in 96-well plates coated with recombinant, murine ICAM-1 (provided by M. Mescher, University of Minnesota, and F. Takei, British Columbia Cancer Agency, Vancouver, Canada) for 10 min at 37°C. Adherent cell number was quantified by fluorescence intensity as previously described (*28*). The results are representative of six independent experiments. **(B)** T cells were stained with fluorochrome-conjugated CD11a (subunit of LFA-1) mAb (Pharmingen) and analyzed by FACS. **(C)** Purified splenic T cells were cultured overnight with anti-CD3ε (2C11, platebound, 5 μg/ml), rested for 5 hours at 37°C, then treated for 2 min with soluble anti-CD3ε, stained with fluorescein-phalloidin (Sigma), and assayed for cellular F-actin (polymerized), as described (*18*). **(D)** LFA-1 clustering on purified T cells was assessed and quantified as described (*9–12*). Typical micrographs of unstimulated and CD3 stimulated cells are shown, and results are expressed as percentages of imaged cells showing polarized LFA-1 distribution (graph). **(E)** Purified splenic T cells were incubated with control Ab- or anti-CD3 (2C11)–coated beads for 20 min, then stained and analyzed by fluorescence microscopy (*9–12*). Typical images of cell-bead contacts (arrows in photomicrographs) are shown. Beads are indicated by asterisks. Results are expressed as the percentage of cell-bead contacts positive for actin or LFA-1 caps (graphs).

ation of the PI-3K effector Akt in SLAP-130/Fyb$^{-/-}$ T cells (*15*). We also examined TCR-dependent increases in polymerized actin (*21*), and found no difference between SLAP-130/Fyb$^{-/-}$ and control T cells (Fig. 3C).

Integrin redistribution into concentrated clusters on T cells after activating stimuli has been reported (*22, 23*). We assessed TCR-stimulated membrane clustering of LFA-1. Purified T cells were left unstimulated or were stimulated with soluble anti-CD3, fixed, stained with fluorochrome-conjugated anti-LFA-1, then evaluated by confocal fluorescence microscopy for evidence of LFA-1 redistribution. Figure 3D (photomicrographs) shows typical "nonpolarized" and "polarized" LFA-1 staining patterns observed in unstimulated or CD3-stimulated, wild-type T cells, respectively. Following anti-CD3 mAb stimulation, we observed a marked increase in the percentage of wild-type T cells displaying the polarized LFA-1 pattern. In contrast, the SLAP-130/Fyb$^{-/-}$ T cells show no TCR-stimulated increase in percentage of cells with polarized LFA-1 (Fig. 3D, graph).

In addition to global redistribution of LFA-1 on the T cell membrane, recent work has suggested that LFA-1 is specifically recruited to a region concentric with aggregated TCR complexes and in proximity to a polymerized actin cap during the formation of an "immunologic synapse" (*24, 25*). To study actin and LFA-1 recruitment in response to a polarizing TCR stimulus, we exposed T cells to beads covalently linked either with anti-CD3 or with control antibody. Fixed cells were stained with phalloidin or with anti–LFA-1, then examined by fluorescence microscopy. We found that, when conjugated with control antibody-coated beads, less than 10% of resting T cells displayed concentration (capping) of polymerized actin or of LFA-1 (Fig. 3E, photomicrographs) at the cell-bead contact site. Contact with anti-CD3 linked beads induced actin or LFA-1 capping (typical cell-bead contacts seen in Fig. 3E, right panels) in greater than 40% of wild-type T cells. SLAP-130/Fyb$^{-/-}$ T cells displayed CD3-bead-specific induction of an actin cap comparable to wild-type cells, yet 50% fewer mutant T cells formed LFA-1 caps in response to bead contact (Fig. 3E, graphs). Taken together, these data indicate that loss of SLAP-130/Fyb uncouples TCR-dependent actin cytoskeletal reorganization from membrane redistribution of LFA-1.

Our data indicate that, although SLAP-130/Fyb is dispensable for the generation of mature T cells and for TCR coupling to proximal signaling events, it has a novel, specific role in the TCR-induced augmentation of integrin activity. Impaired LFA-1 clustering observed following CD3 stimulation of SLAP-130/Fyb–deficient T cells is consistent with previous work documenting a central role for avidity regulation in CD3-induced increases in LFA-1 functional activity on T cells (*26*). The adhesion deficit in SLAP-130/Fyb–deficient cells may also contribute to a failure of cells to proliferate ex vivo in response to a TCR stimulus, as T cell responses are impaired by antagonist antibodies to LFA-1 or ICAM-1, and mice made deficient in LFA-1 display T cell proliferative defects (*27–29*).

SLAP-130/Fyb–deficient T cells reveal that proximal signaling events such as MAPK activation and calcium elevation, while known to be required for TCR-dependent transcriptional activation, are not sufficient to mediate TCR signaling to integrins. Moreover, whereas these PTK-dependent biochemical events display an absolute requirement for the presence of SLP-76 and linker for activated T cells (LAT) (*2, 30*), recent work suggests that these adapters are dispensable for TCR-induced changes in integrin function (*31*). Collectively, these studies and our current observations suggest that SLAP-130/Fyb plays a key role in a TCR-activated pathway parallel with, yet distinct from, the signaling cascades that involve LAT or SLP-76. On the basis of these studies and other work implicating SLAP-130/FYB in vasoactive mediator release (*32*), we propose that SLAP-130/FYB be redesignated Adhesion and Degranulation promoting Adapter Protein (ADAP).

References and Notes

1. L. E. Samelson, *Prog. Biophys. Mol. Biol.* **71**, 393 (1999).
2. D. Yablonski, M. R. Kuhne, T. Kadlecek, A. Weiss, *Science* **281**, 413 (1998).
3. J. L. Clements *et al.*, *Science* **281**, 416 (1998).
4. V. Pivniouk *et al.*, *Cell* **94**, 229 (1998).
5. M. Musci *et al.*, *J. Biol. Chem.* **272**, 11674 (1997).
6. A. da Silva *et al.*, *Proc. Natl. Acad. Sci. U.S.A.* **94**, 7493 (1997).
7. M. Krause *et al.*, *J. Cell Biol.* **149**, 181 (2000).
8. A. J. Hunter, N. Ottoson, N. Boerth, G. A. Koretzky, Y. Shimizu, *J. Immunol.* **164**, 1143 (2000).
9. To generate SLAP-130/Fyb$^{-/-}$ mice, a 10.5-kb PstI genomic fragment containing the SLAP-130 translational start site and first coding exon was isolated from a murine genomic phage library. The 3-kb EcoRI and 1.2-kb EcoRI-PstI genomic fragments served as 5′ and 3′ recombination arms, respectively, and were cloned into the pPNT.neo vector. The targeting vector was electroporated into R1 embryonic stem cells (129/SVJ). G418-resistant embryonic stem cells were injected into day-4 blastocysts and implanted in pseudopregnant mice (InGenious Targeting Laboratory, Stony Brook, NY). Resulting chimeric mice were bred with wild-type B6 to generate animals heterozygous for the targeted allele (*13*).
10. For T cell purification, T cells were negatively selected from red-cell depleted splenocytes using Biomag Sheep anti-FITC particles (Polysciences) after staining with FITC-conjugated anti-B220, anti-Mac-1 (Caltag, each mAb, 10 μl/spleen), and anti-DX-5 (Pharmingen, 5 μl/spleen). Lymph node cells were tumbled with anti-B220 coupled magnetic beads (Dynal). After purification, cell preparations were 88 to 95% CD3-positive.
11. For assessment of LFA-1 clustering, purified splenic T cells were incubated with 2C11 (1 μg/10^6 cells) on ice for 30 min, washed, then cross-linked with goat anti-hamster Ig (0.5 μg/10^6 cells) on ice for 30 min. After further washing, cells were stimulated in 37°C PBS for 10 min, fixed in 4% formaldehyde, stained with anti-CD11a (25 μg/ml, Pharmingen) and plated on poly-L-lysine coated Labtek chamber slides. For each experiment, a minimum of 50 cells from each condition were imaged by confocal microscopy, and analyzed for LFA-1 staining pattern (*33*). Cells were divided into quadrants, fluorescence intensity in each quadrant was determined, and standard deviations (SD) between quadrant fluorescence intensities were calculated. Cells showing SD greater than 0.1 were "polarized," while cells with SD of 0.099 or less were "nonpolarized."
12. For actin and LFA-1 capping studies, antibodies were conjugated with Dynal M450 beads per manufacturer instructions. Cells and beads were co-incubated at a 1:1 ratio for 20 min (RT) and allowed to settle on poly-L-lysine coated glass coverslips. Cells were fixed with 4% paraformaldehyde for 20 min, then blocked with 1:50 normal rat serum in 1% BSA/PBS for 60 min. Samples were stained with either FITC-conjugated anti-mouse CD11a (LFA-1α chain, 50 μg/ml, Pharmingen) mAb or with rhodamine phalloidin (300 nM) for 30 min, washed three times with PBS, and mounted on microscopy slides. Samples were visualized on a Nikon E-800 microscope equipped with CCD camera using fluorescent light with 480/20 nm excitation and 535/25 emission filters. In a blinded fashion, 50 randomly selected cell-bead conjugates per sample were scored as either negative or positive for the presence of an actin or a LFA-1 cap at the cell-bead contact site.
13. Supplemental material is available on *Science* Online at www.sciencemag.org/cgi/content/full/293/5538/2263/DC1.
14. B. D. Freedman, Q. H. Liu, S. Somersan, M. I. Kotlikoff, J. A. Punt, *J. Exp. Med.* **190**, 943 (1999).
15. E. J. Peterson, Q. Liu, B. Freedman, M. Woods, S. Dmowski, Y. Shimizu, G. A. Koretzky, unpublished observations.
16. G. A. Van Seventer, Y. Shimizu, K. J. Horgan, S. Shaw, *J. Immunol.* **144**, 4579 (1990).
17. M. L. Dustin, T. A. Springer, *Nature* **341**, 619 (1989).
18. Y. van Kooyk, P. van de Wiel-van Kemenade, P. Weder, T. W. Kuijpers, C. G. Figdor, *Nature* **342**, 811 (1989).
19. I. Dransfield, C. Cabanas, A. Craig, N. Hogg, *J. Cell Biol.* **116**, 219 (1992).
20. T. Zell, W. J. Kivens, S. A. Kellermann, Y. Shimizu, *Immunol. Res.* **20**, 127 (1999).
21. J. Zhang *et al.*, *J. Exp. Med.* **190**, 1329 (1999).
22. Y. van Kooyk, P. Weder, K. Heije, C. G. Figdor, *J. Cell Biol.* **124**, 1061 (1994).
23. M. P. Stewart, A. McDowall, N. Hogg, *J. Cell Biol.* **140**, 699 (1998).
24. A. Grakoui *et al.*, *Science* **285**, 221 (1999).
25. C. R. Monks, B. A. Freiberg, H. Kupfer, N. Sciaky, A. Kupfer, *Nature* **395**, 82 (1998).
26. M. P. Stewart, C. Cabanas, N. Hogg, *J. Immunol.* **156**, 1810 (1996).
27. R. Schmits *et al.*, *J. Exp. Med.* **183**, 1415 (1996).
28. C. Berlin-Rufenach *et al.*, *J. Exp. Med.* **189**, 1467 (1999).
29. K. Scharffetter-Kochanek *et al.*, *J. Exp. Med.* **188**, 119 (1998).
30. W. Zhang, J. Sloan-Lancaster, J. Kitchen, R. P. Trible, L. E. Samelson, *Cell* **92**, 83 (1998).
31. J. A. Epler, R. Liu, H. Chung, N. C. Ottoson, Y. Shimizu, *J. Immunol.* **165**, 4941 (2000).
32. L. Geng, S. Pfister, S.-K. Kraeft, C. E. Rudd, *Proc. Natl. Acad. Sci. U.S.A.*, in press.
33. P. Reichert, R. L. Reinhardt, E. Ingulli, M. K. Jenkins, *J. Immunol.* **166**, 4278 (2001).

34. The authors acknowledge F. High and E. Chung, University of Pennsylvania, and B. Yang, R. Williamson, and R. Hrstka, University of Iowa Gene Targeting Laboratory, for technical assistance. B. Schraven and M. Kahn provided critical discussion. Supported by the Abramson Family Cancer Research Institute (G.A.K.), the NIH (E.J.P., M.L.W., M.S.J., B.D.F., Y.S., and G.A.K.), and the American Heart Association (J.T.P. and P.S.M.).

15 June 2001; accepted 27 July 2001